Electronic Supplementary Information

A naphthalimide based PET probe with Fe^{3+} selective detection ability: Theoretical and experimental study

Narendra Reddy Chereddy,*[a] M. V. Niladri Raju,[a] Peethani Nagaraju,[a] Venkat Raghavan Krishnaswamy,[b] Purna Sai Korrapati,[b] Prakriti Ranjan Bangal*[c] and Vaidya Jayathirtha Rao*[a]

[a]*Crop Protection Chemicals Division,* [c]*Inorganic and Physical Chemistry Division, CSIR-Indian Institute of Chemical Technology, Tarnaka, Hyderabad-500 007, India.*
[b]*Biomaterials Division, CSIR-Central Leather Research Institute, Adyar, Chennai-600 020, India*

Corresponding author Tel.: +91 40 27193933; Fax: +91 44 27193382
E-Mail: chereddynarendra@gmail.com

Table of contents **Page**

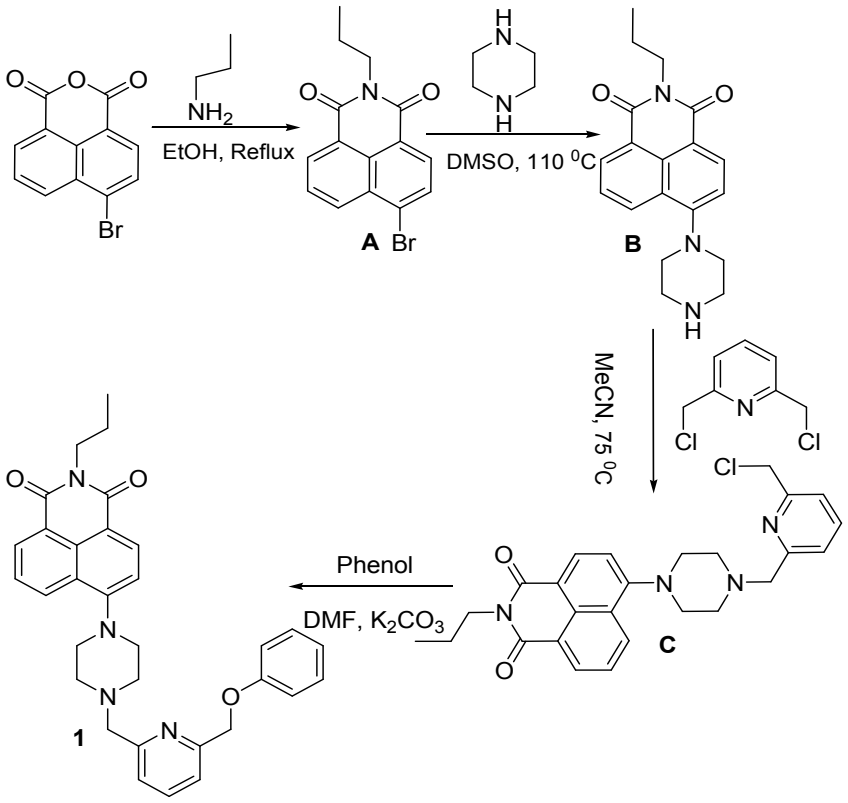

Scheme S1. Synthesis of naphthalimide probe **1**

General Information

Dry acetonitrile and double distilled water were used in all experiments. All the materials for synthesis were purchased from commercial suppliers and used without further purification. The W138 (normal lung fibroblast) cells from American Type Culture Collection (Manassas, VA). Dulbecco's Modified Eagle Medium (DMEM), Dulbecco's Phosphate Buffered Saline (DPBS), Hank's Balanced Salt Solution (HBSS), Fetal Bovine Serum (FBS), and penicillin/streptomycin were purchased from Sigma-Aldrich, USA. The solutions of metal ions were prepared from the corresponding chloride salts. Absorption spectra were recorded on a Cary 5000 UV-Vis-NIR spectrophotometer. Fluorescence measurements were performed on a Cary Eclipse fluorescence spectrophotometer (Excitation wavelength 400 nm; excitation, emission slit widths are 5 nm each). All pH measurements were made with a Systronics μpH System Model 361. NMR spectra were recorded using a Bruker 300 and 500 MHz NMR spectrometers. ESI-High-resolution mass spectrum (HRMS) was recorded on QSTAR XL Hybrid MS/MS mass spectrometer. All measurements were carried out at room temperature. Stock solution of the probe was prepared by dissolving 5.20 mg of **1** in 1:1 v/v

0.01M Tris HCl-CH_3CN (pH 7·4) and making up to the mark in a 10 mL volumetric flask. Further dilutions were made to prepare 25 μM solutions for the experiments. Stock solutions of metal ions (1 M) were prepared in de-ionised water.

Synthesis of probe 1

To a solution of 4-bromo-1,8-naphthanoic anhydride (1.00 g, 3.60 mmol) in ethanol maintained at 70 ^{0}C, propylamine (1.0 mL) was added slowly. The resulting mixture was stirred for ~2h, cooled to room temperature and precipitate formed (**A**) was filtered, used in the next step. To this product **A**, (0.70 g, 2.20 mmol) in DMSO, piperazine (1.00 g, 11.6 mmol) and K_2CO_3 (0.42 g, 3.0 mmol) were added and stirred at 110 ^{0}C for 3h. After completion, the reaction mixture was extracted with DCM and subjected to column chromatography (silica gel 100-200 mesh) and eluted using ethtyl acetate to get 0.50 g (70%) of **B**. To 4-piperazinyl-N-propyl-1,8-naphthanamide, **B**, (0.48 g, 1.5 mmol) in acetonitrile (20 mL), 2,6-Bis(chloromethyl)pyridine (0.71 g, 4.0 mmol) was added and the mixture was refluxed overnight under N_2 atmosphere. After completion of the reaction, the reaction mixture was cooled to room temperature, concentrated and subjected to column chromatography (silica gel 100-200 mesh, 1:9 ethyl acetate-hexane as eluent) to afford **C** (0.44 g, 64%) as pale yellow solid. To the mixture of **C** (0.61 g, 1.0 mmol) and potassium carbonate (0.28 g, 2.0 mmol) in DMF, phenol (0.15 g, 1.5 mmol) was added and the mixture was stirred at room temperature over night. After completion, the reaction mixture was partitioned between chloroform and water, chloroform layer was collected. The aqueous layer was washed thrice with chloroform (3 x 10 mL) and the combined organic extract was washed with brine, concentrated and subjected to column chromatography to afford **1** in pure form (0.40 g, 78%). ^{1}H NMR (400 MHz, $CDCl_3$, δ ppm): 1.00 (t, *J* = 7.2 Hz, 3H), 1.75 (q, *J* = 7.6 Hz, 2H), 2.88 (s, 4H), 3.33 (s, 4H), 3.85 (s, 2H), 4.13 (t, *J* = 7.6 Hz, 2H), 5.23 (s, 2H), 6.90-7.11 (m, 3H), 7.21 (d, *J* = 7.6 Hz, 1H), 7.24-7.33 (m, 1H), 7.40-7.51 (m, 2H), 7.62-7.77 (m, 2H), 8.01 (s, 1H), 8.41 (d, *J* = 8.4 Hz, 1H), 8.50 (d, *J* = 8.0 Hz, 1H), 8.56 (d, *J* = 7.2 Hz, 1H). ^{13}C NMR (100 MHz, $CDCl_3$, δ ppm): 11.55, 21.42, 31.44, 36.50, 41.77, 53.01, 53.38, 64.39, 70.55, 114.79, 114.89, 116.72, 119.80, 121.14, 122.18, 123.26, 125.61, 126.13, 129.54, 129.85, 130.27, 131.06, 132.52, 137.35, 155.93, 156.97, 157.67, 158.38, 162.56, 164.04, 164.50. ESI-HRMS (+ve mode, m/z): 521.25282 ($M+H^+$), Calc. for $C_{32}H_{33}N_4O_3$ is 521.25527.

Sample preparation for cell culture

The solution of **1** was prepared in sterile DMSO solvent with stock solution concentrations of 10 mM. Similarly, 10 mM stock solution of Fe^{3+} salts was prepared in sterile Millipore water. The freshly prepared stock solutions of each sample were used for cell culture experiment.

Cell culture experimentation

W138 cells were maintained in DMEM complete media, supplemented with 10% Fetal Bovine Serum (FBS) and 1% penicillin/streptomycin at 37 ^{0}C humidified incubator with 5% CO_2. Cells after 70% confluency were seeded into 96 well plate and 24 well plate for cyto-toxicity assays and fluorescence microscopy studies, respectively.

MTT assay

The MTT (3-(4,5-dimethylthiazol-2-yl)-2,5-diphenyl tetrazolium bromide) assay has been used to measure the activity of enzymes that reduce MTT to formazan dyes, giving rise to a purple colour. Briefly, 10,000 of NIH 3T3 cells were plated in each well of a 96-well tissue culture plate with 100 μL of complete DMEM media at 37 ^{0}C humidified incubator with 5% CO_2 for 24 h. Next day, the media was replaced with 100 μL (in each well) fresh media and the cells were incubated with probe **1** at different concentrations (0.1-25 μM) for another 48 h. 1 mL of MTT stock solution (5 mg/mL) was diluted to 10 mL using complete DMEM media and 100 μL of the diluted MTT solution was added to each well of 96 well plate by replacing the old media and allowed to incubate for 4 h. After that, the media in each well was replaced by 100 μL of 1:1 DMSO-Methanol mixture (v/v) for solubilizing the purple formazan product. Then, the plate was kept on a shaker for homogeneous mixture of the solution. Finally, the microplate reader (ELx 800 MS) has been used to measure the absorbance of solution in each well of the plate at 570 nm.

Fluorescence microscopy

To conduct live cell imaging experiments, W138 cells were seeded at $2x10^4$ cells/mL/well in a 24-well tissue culture plate for 24 h at 37 ^{0}C humidified incubator with 5% CO_2 in complete DMEM media. After 24 h, the cells were incubated with probe **1** (10 μM) for another 4 h. The cells were thoroughly washed with DPBS for six times to eradicate the unbound probe **1** from the surface of cell membrane. After that, the cells treated with probe **1** were incubated with 10 μM of Fe^{3+} ions for 1 h. Additionally, cells were also treated with only **1** (10 μM), and only Fe^{3+} (10 μM) solutions and again washed with DPBS for six times to remove the unbound materials. Finally, the fluorescence images of W138 cells treated with probe **1** and **1**

and Fe^{3+}, only probe **1** and only Fe^{3+} were observed under fluorescence microscope (Leica DM IRB microscope equipped with EBQ-100 UV-lamp) through the green (Emission filter LP 515) channel.

Fluorescence measurements using well plate reader

Human lung fibroblast, W138 cells, were cultured as described above and plated at a density of 5 x 10^4 cells/ well in a 12 well black with transparent bottom tissue culture plate. The cells were allowed adhere and spread overnight in the medium supplemented with FBS and antibiotics. Next day, the cells were washed twice with PBS and treated with 10 μM probe for 4 hours. The cells were again washed with PBS and treated with different concentration Fe^{3+} (0-10 μM) for 1 hour. The intensity of the fluorescence emitted was measured using a micro plate reader (Tecan Infinite M200 PRO) with excitation and emission wavelengths of 400 and 515 nm, respectively.

Theoritical studies

Density functional theory studies were carried out on two molecules **1** and its Iron complex **(1-Fe)$^{3+}$** using Gaussian 03 software.[1] The complex was treated as open shell system using spin unrestricted DFT wave functions because iron atom exits in the form of Fe(III) in its complex. Geometry optimization have been carried out using B3LYP functional[2] and 6-31G(D,P) basis set for **1** and **(1-Fe)$^{3+}$**. For iron atom as it is in the form of Fe(III), low spin state of 1/2 was considered for our calculations. Frequency calculations are performed on the same level of theory to ensure no imaginary frequencies are present to confirm the optimized geometry is the local minima on potential energy surface. TD-DFT analysis was done at B3LYP functional and 31G(D,P) basis set to get a deeper understanding of the electronic transitions in the PET quenching process.

TSCPC experiments

The femtosecond pulses at required repetition rate were obtained from fractional part of MaiTai output passing through femtosecond Pulse Selector (3980-5S, Spectra Physics, single shot to 8 MHz). The excitation pulses at desired wavelength were generated by frequency doubling with 0.5 mm BBO crystal. This excitation pulses are focused to the sample using our Fluorescence Up-conversion set up (FOG100 system CDP System). The time distribution data of fluorescence intensity were recorded on a SPC-130 TCSPC module (Becker & Hickl).

ICP-OES analysis

Sample preparation for ICP-OES analysis was carried out as described elsewhere.[3] The W138 cells used for well plate reader analysis were collected and concentrated nitric acid (100 µL) was added to each sample and heated for 2 h at 90 °C. To the above samples H_2O_2 (25 µL) was added and heated for another 2 h at 90 °C, after which concentrated hydrochloric acid (40 µL) was added and digested overnight at room temperature. The resultant solution was diluted 50 mL with 1% HNO_3 and subjected to ICP-OES analysis. Analysis was carried out on an iCAP 6500 Duo ICP spectrometer (Thermo Scientific) operated at 1 L/min nebulizer argon pressure and 1150 W RF forward power. The instrument had been calibrated using 0, 2.5, 5.0, and 10.0 ppm of an Iron ICP standard solution (Merck, Germany).

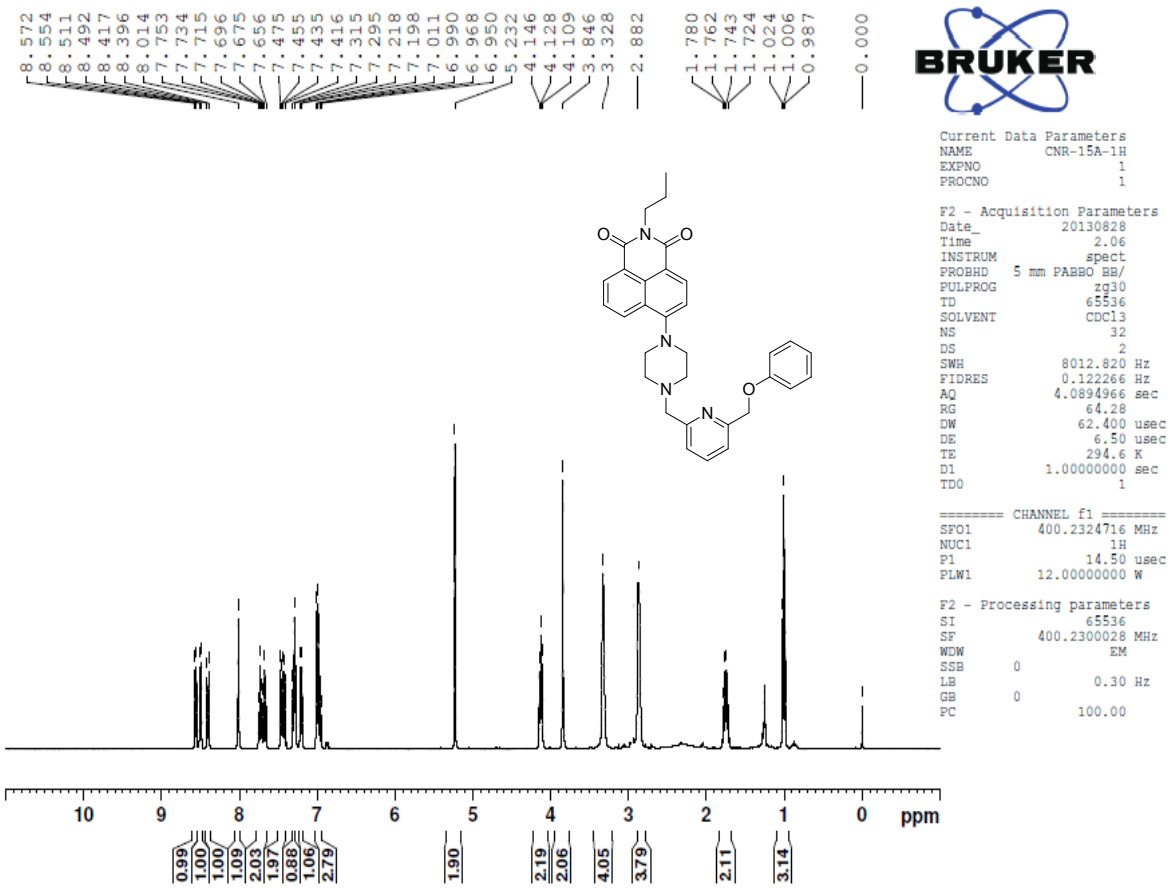

Fig. S1. ^{1}H NMR spectrum of **1** in $CDCl_3$

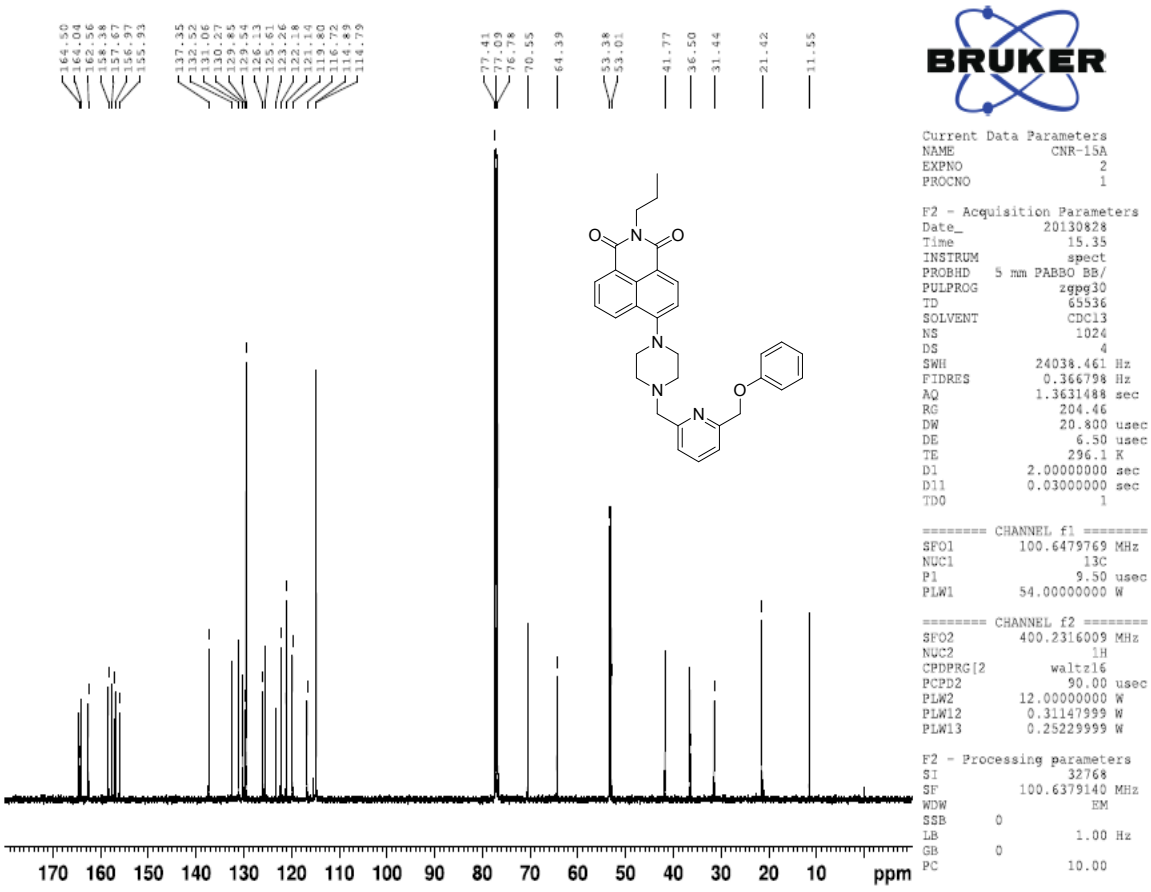

Fig. S2. ^{13}C NMR spectrum of **1** in $CDCl_3$

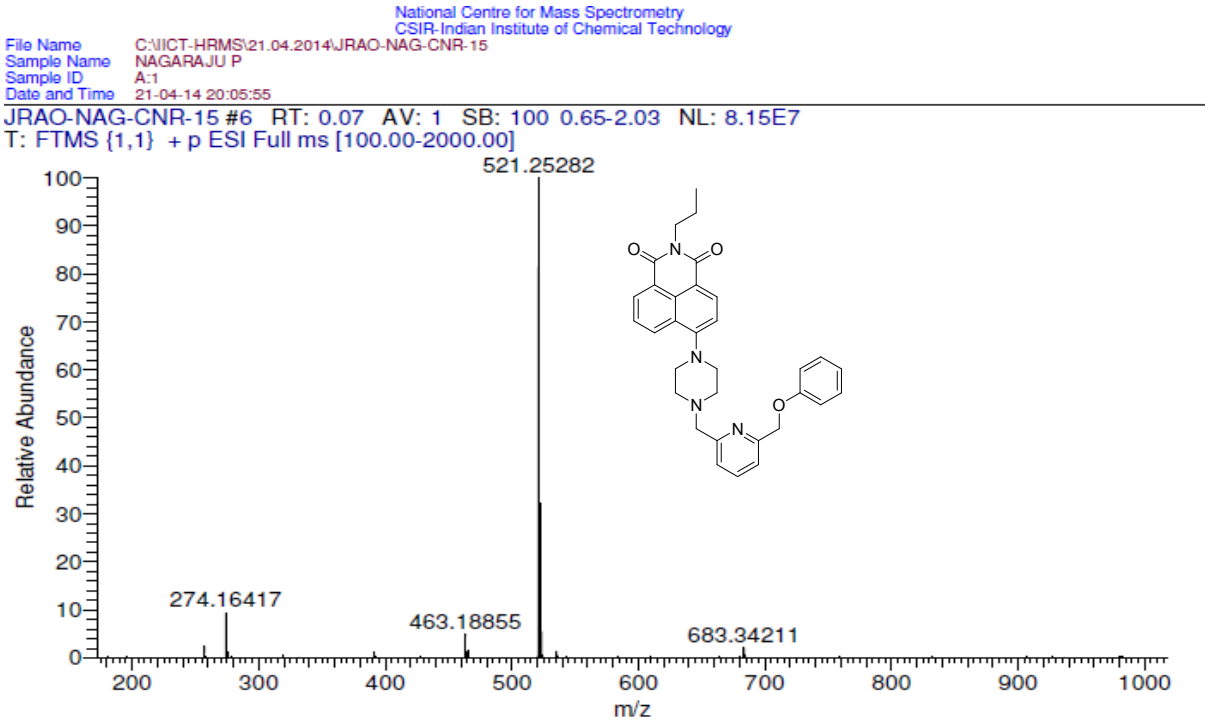

JRAO-NAG-CNR-15#17-38 RT: 0.22-0.51 AV: 22
T: FTMS {1,1} + p ESI Full ms [100.00-2000.00]
m/z= 497.40-566.41

m/z	Intensity	Relative	Theo. Mass	Delta (ppm)	RDB equiv.	Composition
521.25301	1753713.5	100.00	521.25472	-3.27	18.5	$C_{32}H_{33}O_3N_4$
522.25641	569985.7	32.50				

Fig. S3. ESI High resolution mass spectrum of **1**

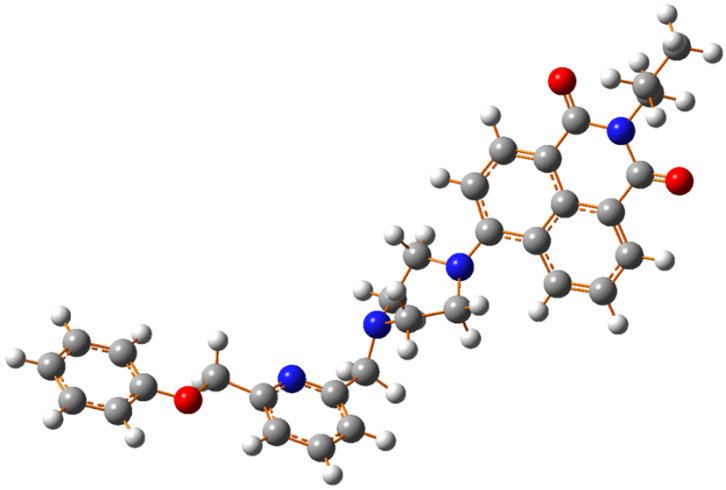

B3LYP/6-31G(D,P) optimized geometry of **1**

B3LYP/6-31G(D,P) optimized geometry co-ordinates of **1**

	X	Y	Z
C	5.82514781	-2.00772447	-1.34109444
C	4.64822532	-2.77851906	-1.33457635

C	3.47379306	-2.25916891	-0.82415196
C	3.41914315	-0.94028948	-0.30628319
C	4.63110017	-0.18583109	-0.25801805
C	5.82218172	-0.73428299	-0.79918514
C	2.21259091	-0.35387500	0.22212927
C	2.29180067	0.88222292	0.85708433
C	3.50119095	1.59292502	0.92906830
C	4.65716235	1.09017859	0.36065907
C	5.90507093	1.88000059	0.41930072
N	7.03930468	1.31612757	-0.19114852
C	7.08723740	0.04344681	-0.77615359
C	8.28634897	2.10155038	-0.16790653
O	8.13297314	-0.39151936	-1.24396589
O	5.97134599	2.97736906	0.96106429
N	1.00161476	-1.06692810	0.11169379
C	9.14006539	1.82282829	1.07378912
C	10.42884377	2.64948569	1.07217264
C	0.44504775	-1.21134759	-1.24789653
C	-0.06286392	-0.74446891	1.06379427
C	-0.63095767	-2.29343316	-1.26636447
N	-1.68547576	-1.97769830	-0.30725241
C	-1.12810548	-1.83960510	1.03581773
C	-2.79118362	-2.93427734	-0.37250600
C	-4.03479521	-2.44717020	0.34668510
C	-4.47459510	-3.04302830	1.53376678
C	-5.62974329	-2.55491479	2.14257553
C	-6.30947289	-1.49235757	1.55348318
C	-5.79715618	-0.96350688	0.36501331
N	-4.69031775	-1.42723776	-0.22711077
C	-6.45264857	0.18611649	-0.36816712
O	-7.62610018	0.58337856	0.32242337
C	-8.36623759	1.61789603	-0.18322826
C	-8.04802288	2.32384350	-1.34865551
C	-8.88253392	3.36466922	-1.76871935
C	-10.02187619	3.70650152	-1.04498423
C	-10.33067229	2.99416209	0.11871574
C	-9.51205233	1.95696455	0.55020552
H	6.75459219	-2.39689661	-1.74229372
H	4.66881928	-3.79378997	-1.71828074
H	2.58149824	-2.87294977	-0.77893122
H	1.39862205	1.33270691	1.27306443
H	3.54215471	2.56603912	1.40693443
H	7.99715524	3.15285657	-0.20040857
H	8.83876721	1.84459163	-1.07299033
H	9.38061471	0.75428380	1.10387201
H	8.54833806	2.05240143	1.96697569
H	11.03064303	2.44149099	1.96212401

H	10.21280414	3.72370532	1.06107170
H	11.04486922	2.42382153	0.19451304
H	1.24393042	-1.46634964	-1.94569296
H	-0.00004819	-0.25765890	-1.57674439
H	-0.54517394	0.22034999	0.83173343
H	0.36916446	-0.67990146	2.06639600
H	-0.16103656	-3.27629011	-1.05942605
H	-1.07016526	-2.34099521	-2.26908387
H	-1.93094578	-1.56957159	1.72867972
H	-0.67915561	-2.78747088	1.39391482
H	-2.50236739	-3.92710997	0.02345541
H	-3.04608019	-3.06581437	-1.42929966
H	-3.92160660	-3.87173014	1.96517738
H	-5.99549753	-2.99774663	3.06457569
H	-7.21191738	-1.07942918	1.98578185
H	-6.68890293	-0.13034232	-1.39380140
H	-5.73948549	1.01949022	-0.43986507
H	-7.16755365	2.07752686	-1.92964445
H	-8.62955248	3.90844106	-2.67443218
H	-11.21597582	3.24845551	0.69440621
H	-9.73750386	1.39443342	1.45031119
H	-10.66283605	4.51583731	-1.37976049

Fig. S4. Energetically optimized structure and its corresponding Cartesian coordinates of **1**

Table 1: Calculated dominant electronic transition wavelengths with oscillator strength of **1** and **1-Fe^{3+}**

1		**1-Fe^{3+}**	
Transition	Wavelength (nm) (Oscillator strength)	Transition	Wavelength (nm) (Oscillator strength)
HOMO → LUMO (0.64362) HOMO-3 → LUMO (0.12171)	386.44 nm (f=0.2744)	HOMO-12 → LUMO (0.82623)	502.15 nm f=0.2037
HOMO → LUMO+2 (0.37342) HOMO-9 → LUMO (0.31948)	253.52 nm f=0.1532	HOMO-2 → LUMO (0.58392)	339.13 nm f=0.1883

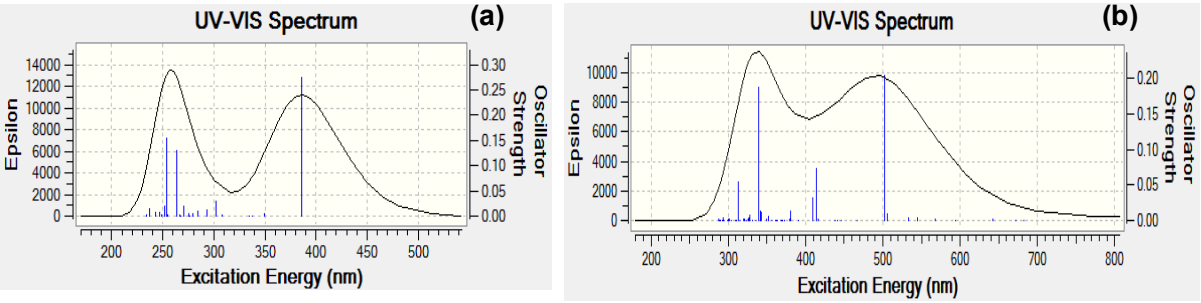

Fig. S5. Theoretically generated absorption spectrum of **1** (**a**) and **1-Fe^{3+}** complex (**b**)

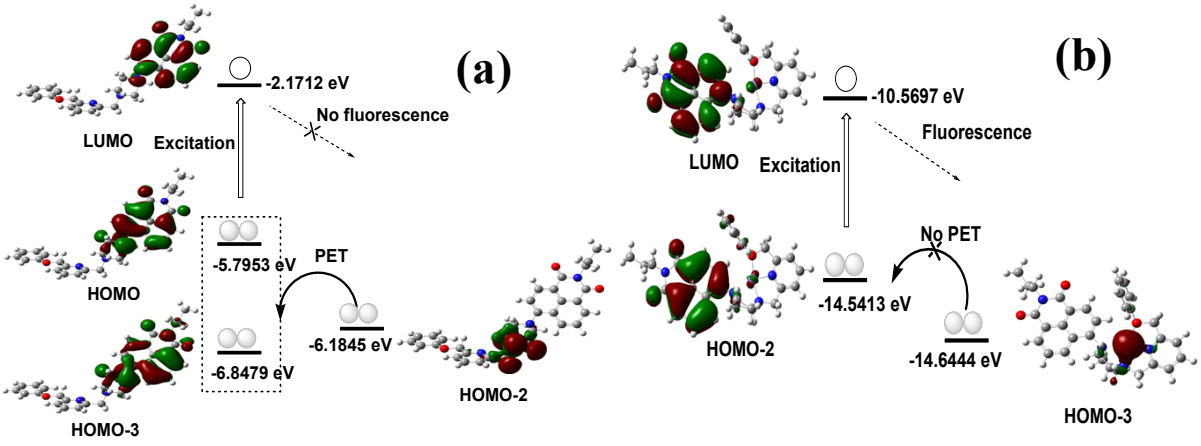

Fig. S6. TD-DFT results of **1** (**a**) and **1-Fe^{3+}** complex (**b**).

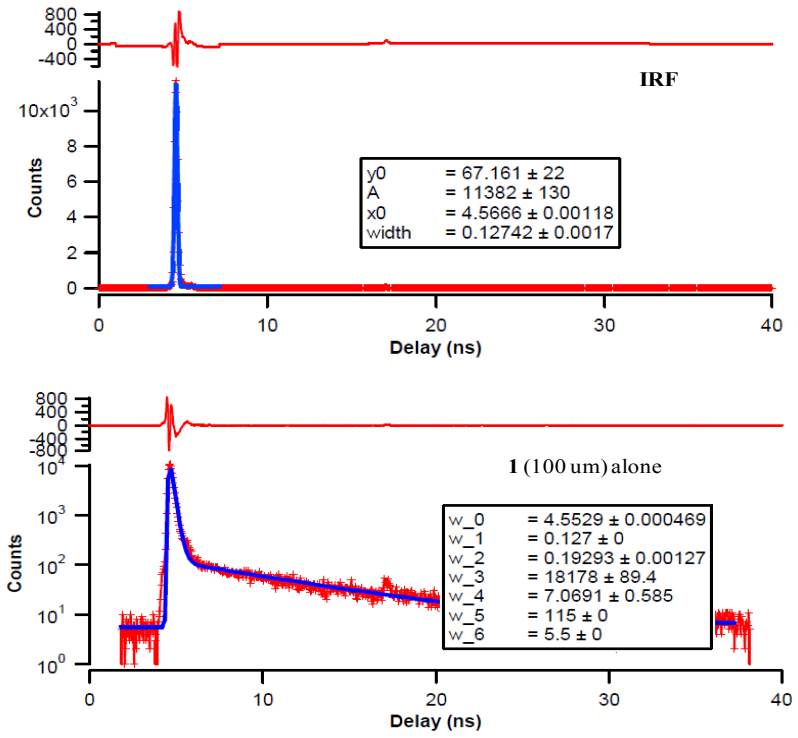

Fig. S7. The instrument response function (top) and nono-second fluorescence decay profile (bottom) of **1**

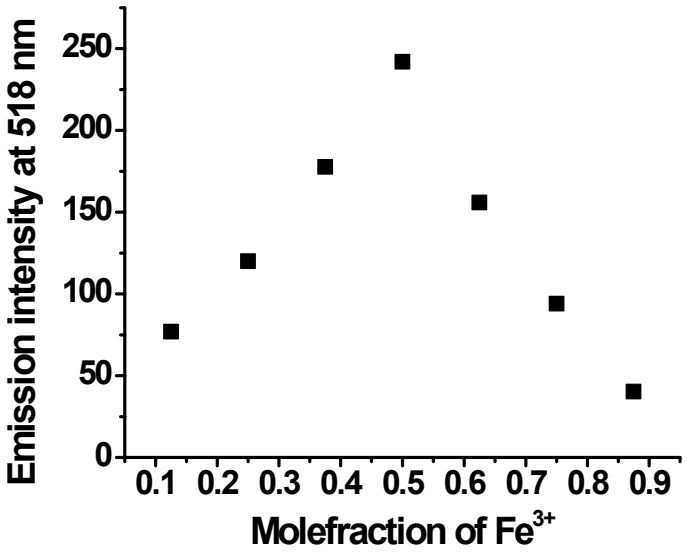

Fig. S8. Job plot of 1:1 complex of **1** and Fe^{3+} in 1:1 v/v 0.01 M Tris HCl-CH_3CN, pH 7.4, the emission at 518 nm was plotted against the mole fraction of Fe^{3+} ions. The total concentration of Fe^{3+} ions with **1** was 20 μM.

Fig. S9. ESI-MS spectrum of **1**-Fe^{3+} complex

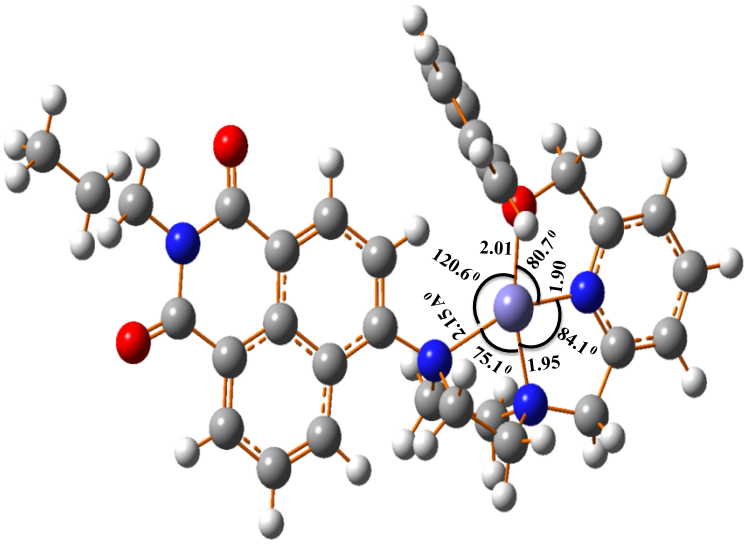

B3LYP/6-31G(D,P) optimized geometry of **(1-Fe)$^{3+}$** complex

B3LYP/6-31G(D,P) optimized geometry co-ordinates of **(1-Fe)$^{3+}$** complex

	X	Y	Z
C	-4.10886178	-3.13378480	0.67528315
C	-2.87046796	-3.78984977	0.76152367
C	-1.69475240	-3.09691223	0.55496617
C	-1.67245363	-1.70487471	0.24869334
C	-2.94813560	-1.04291164	0.14234901
C	-4.14576358	-1.78261421	0.36929298
C	-0.49122496	-0.90979730	0.01445366
C	-0.60881289	0.41369720	-0.35107364
C	-1.85728159	1.04540625	-0.46605082
C	-3.01262977	0.33329207	-0.20990271
C	-4.29849368	1.04647027	-0.32029052
N	-5.49298865	0.29206452	0.02119936
C	-5.47039167	-1.14835827	0.28427744
C	-6.73262260	0.94473720	0.00888956
O	-6.53394364	-1.70816100	0.41924039
O	-4.42847583	2.20295453	-0.65843900
N	0.89094654	-1.43236381	0.09594343
C	1.22882369	-2.01812561	1.45469372
C	1.14605620	-2.44134245	-1.00739831
C	2.60622878	-2.71352501	1.36991860
N	3.29462768	-2.16960564	0.15835106
C	2.65593384	-2.77162683	-1.05745925
C	4.79362894	-2.30369731	0.14477796
C	5.40318838	-1.03023294	-0.39977120
C	6.72278287	-0.86838841	-0.79485245
C	7.15258015	0.40752268	-1.18203573

C	6.27038098	1.49095400	-1.16018937
C	4.95843911	1.26311843	-0.75995728
N	4.55233840	0.02786009	-0.40729785
C	3.89028855	2.31681744	-0.65554874
O	2.66449793	1.68619139	-0.13093977
C	1.79373302	2.64426445	0.49456857
C	1.09059198	3.53835861	-0.30702836
C	0.28222280	4.48996564	0.32167272
C	0.19011182	4.52631219	1.71586951
C	0.90895002	3.61591678	2.49399070
C	1.73161740	2.66472043	1.88323251
H	-5.03755214	-3.66980408	0.83988936
H	-2.83962955	-4.84972966	0.98937649
H	-0.77638260	-3.66191174	0.62289926
H	0.28269943	0.98955676	-0.54929141
H	-1.92007292	2.09159075	-0.74302246
H	-6.60796818	2.01218675	0.18247759
H	-7.44143981	0.42847303	0.65544086
H	0.46874972	-2.71489521	1.80530803
H	1.24548831	-1.18647873	2.16478928
H	0.81362215	-1.99136188	-1.94409094
H	0.55698558	-3.34577934	-0.84987127
H	2.51857676	-3.80274947	1.28746107
H	3.19911331	-2.49044243	2.25836250
H	3.13253845	-2.35201709	-1.94717277
H	2.83015417	-3.85356124	-1.06406390
H	5.09773819	-3.18616192	-0.42726229
H	5.13634249	-2.45384251	1.17387762
H	7.40928446	-1.70840689	-0.79549061
H	8.18178365	0.55713636	-1.49318454
H	6.60072708	2.48431949	-1.44489274
H	3.66227471	2.76473604	-1.62767313
H	4.18372873	3.10989842	0.03825173
H	1.17707835	3.50827420	-1.38899883
H	-0.26218768	5.20989370	-0.28066168
H	0.85131541	3.65754175	3.57658561
H	2.33036117	1.98152965	2.47868204
Fe	2.72247337	-0.30500918	-0.04423798
H	-0.43009392	5.27529386	2.19676551
C	-7.44743459	0.85066343	-1.51808313
H	-6.72152046	1.32647751	-2.18129702
H	-7.52801024	-0.22208682	-1.70597835
C	-8.77485133	1.55779299	-1.46370315
H	-9.20267415	1.46964881	-2.47884956
H	-9.48571767	1.09024405	-0.77826085
H	-8.68899915	2.62528977	-1.24683397

Fig. S10. Energetically optimized structure and its corresponding Cartesian coordinates of **(1-Fe)$^{3+}$** complex.

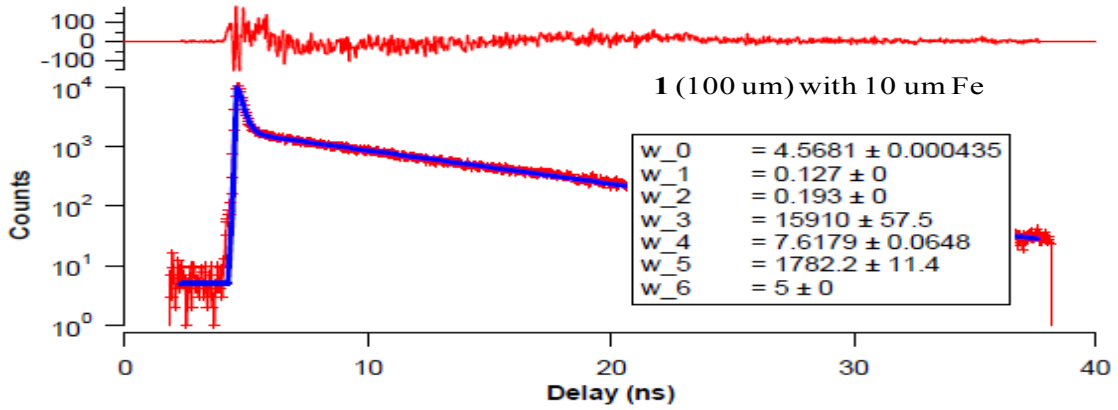
1 (100 um) with 10 um Fe
w_0 = 4.5681 ± 0.000435
w_1 = 0.127 ± 0
w_2 = 0.193 ± 0
w_3 = 15910 ± 57.5
w_4 = 7.6179 ± 0.0648
w_5 = 1782.2 ± 11.4
w_6 = 5 ± 0
Counts
Delay (ns)

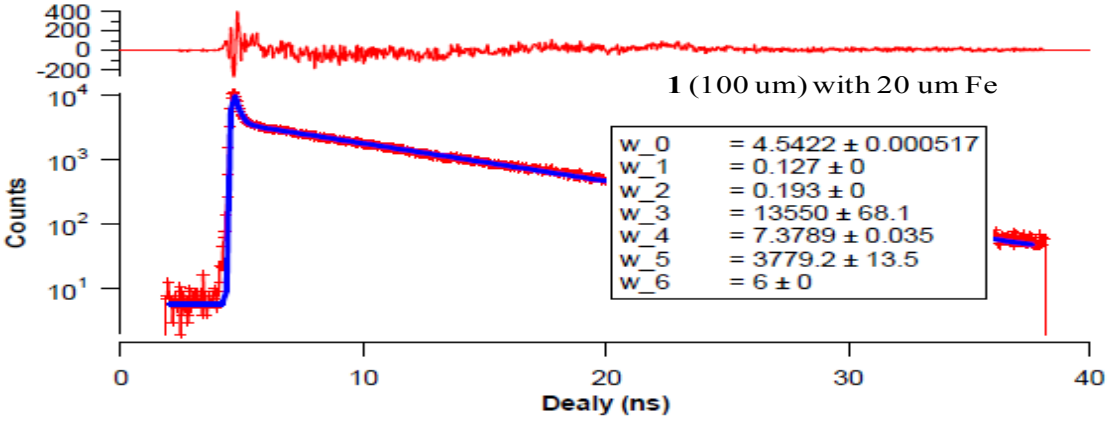
1 (100 um) with 20 um Fe
w_0 = 4.5422 ± 0.000517
w_1 = 0.127 ± 0
w_2 = 0.193 ± 0
w_3 = 13550 ± 68.1
w_4 = 7.3789 ± 0.035
w_5 = 3779.2 ± 13.5
w_6 = 6 ± 0
Counts
Dealy (ns)

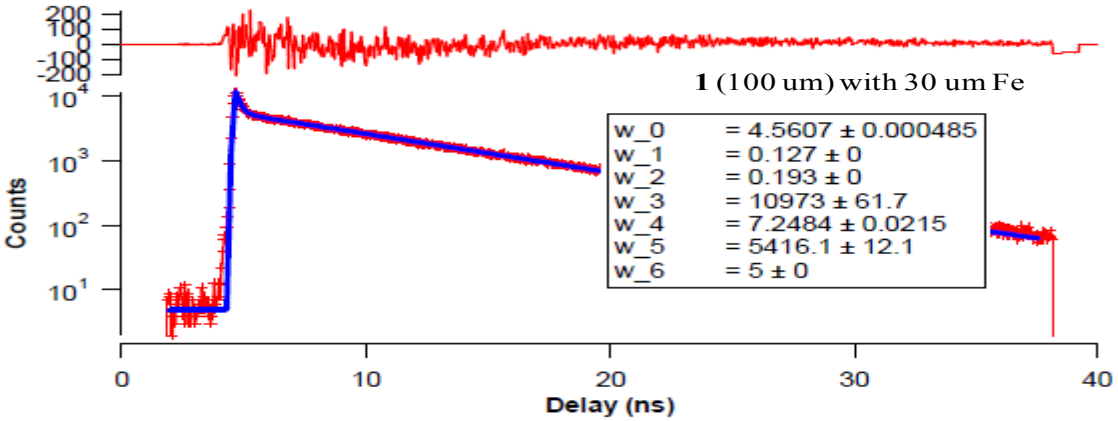
1 (100 um) with 30 um Fe
w_0 = 4.5607 ± 0.000485
w_1 = 0.127 ± 0
w_2 = 0.193 ± 0
w_3 = 10973 ± 61.7
w_4 = 7.2484 ± 0.0215
w_5 = 5416.1 ± 12.1
w_6 = 5 ± 0
Counts
Delay (ns)

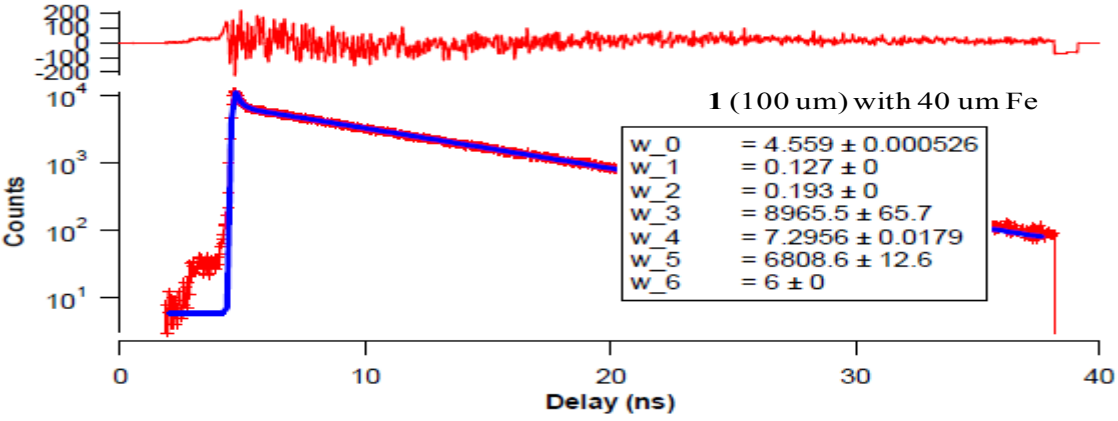
1 (100 um) with 40 um Fe
w_0 = 4.559 ± 0.000526
w_1 = 0.127 ± 0
w_2 = 0.193 ± 0
w_3 = 8965.5 ± 65.7
w_4 = 7.2956 ± 0.0179
w_5 = 6808.6 ± 12.6
w_6 = 6 ± 0
Counts
Delay (ns)

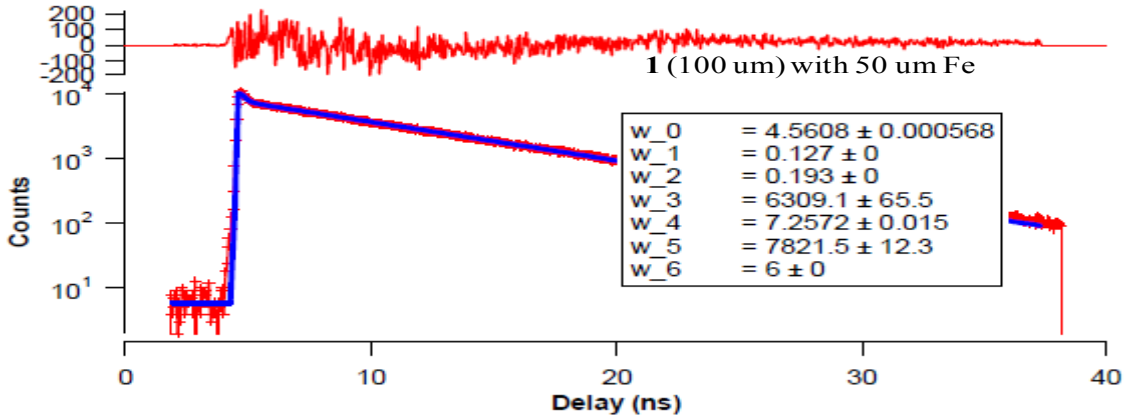
1 (100 um) with 50 um Fe
w_0 = 4.5608 ± 0.000568
w_1 = 0.127 ± 0
w_2 = 0.193 ± 0
w_3 = 6309.1 ± 65.5
w_4 = 7.2572 ± 0.015
w_5 = 7821.5 ± 12.3
w_6 = 6 ± 0
Counts
Delay (ns)

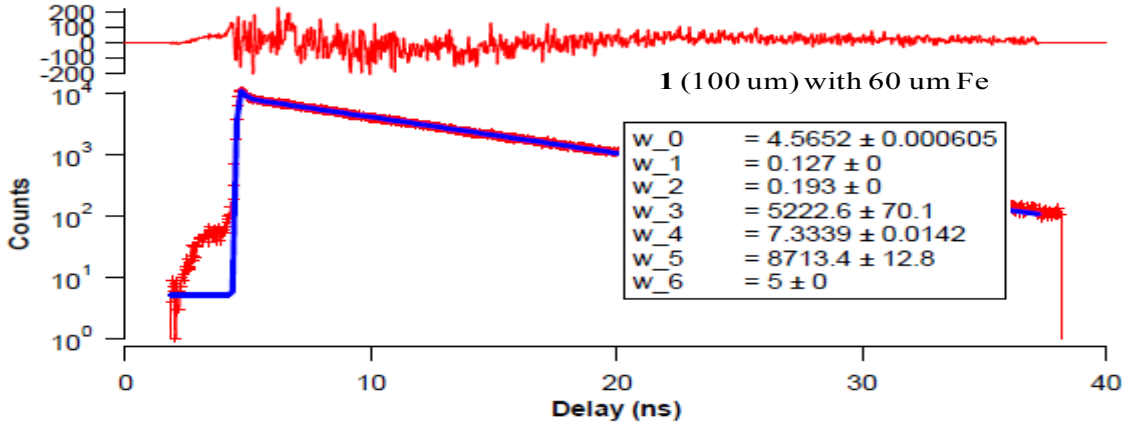
1 (100 um) with 60 um Fe
w_0 = 4.5652 ± 0.000605
w_1 = 0.127 ± 0
w_2 = 0.193 ± 0
w_3 = 5222.6 ± 70.1
w_4 = 7.3339 ± 0.0142
w_5 = 8713.4 ± 12.8
w_6 = 5 ± 0
Counts
Delay (ns)

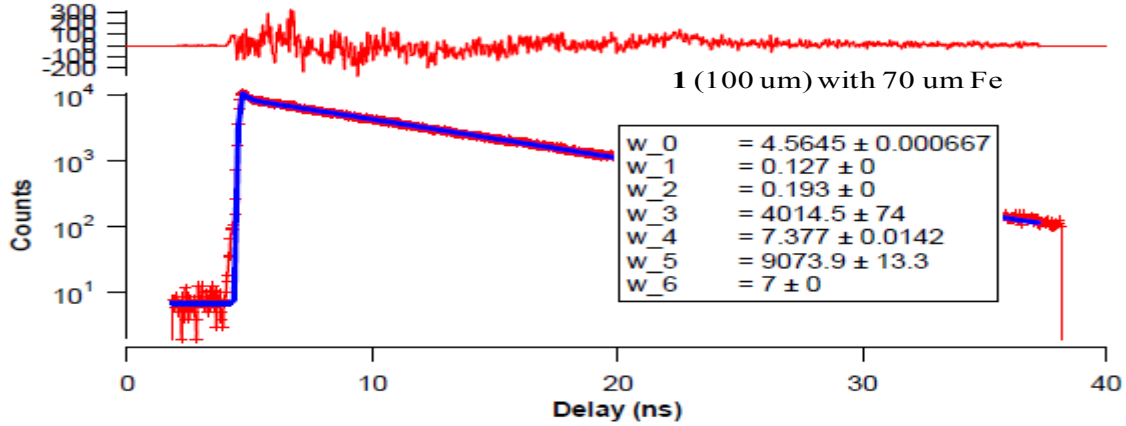
1 (100 um) with 70 um Fe
w_0 = 4.5645 ± 0.000667
w_1 = 0.127 ± 0
w_2 = 0.193 ± 0
w_3 = 4014.5 ± 74
w_4 = 7.377 ± 0.0142
w_5 = 9073.9 ± 13.3
w_6 = 7 ± 0
Counts
Delay (ns)

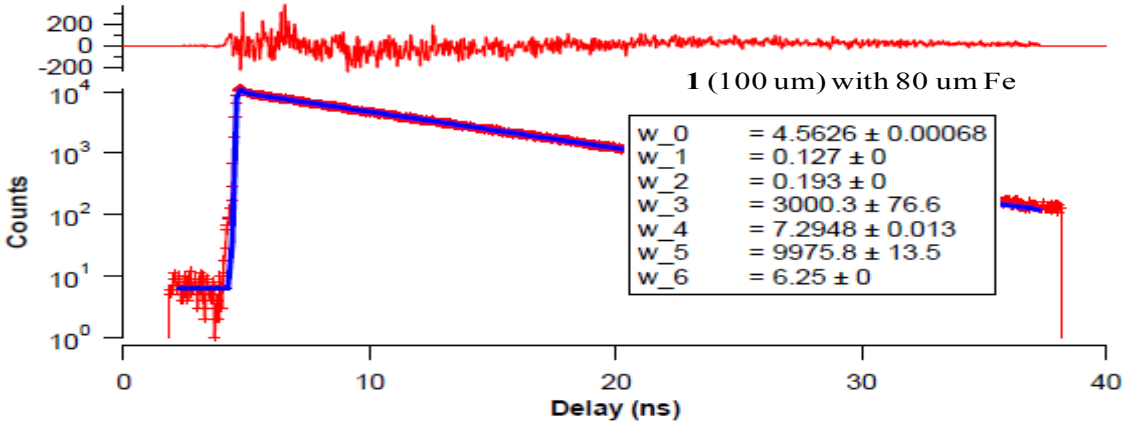
1 (100 um) with 80 um Fe
w_0 = 4.5626 ± 0.00068
w_1 = 0.127 ± 0
w_2 = 0.193 ± 0
w_3 = 3000.3 ± 76.6
w_4 = 7.2948 ± 0.013
w_5 = 9975.8 ± 13.5
w_6 = 6.25 ± 0
Counts
Delay (ns)

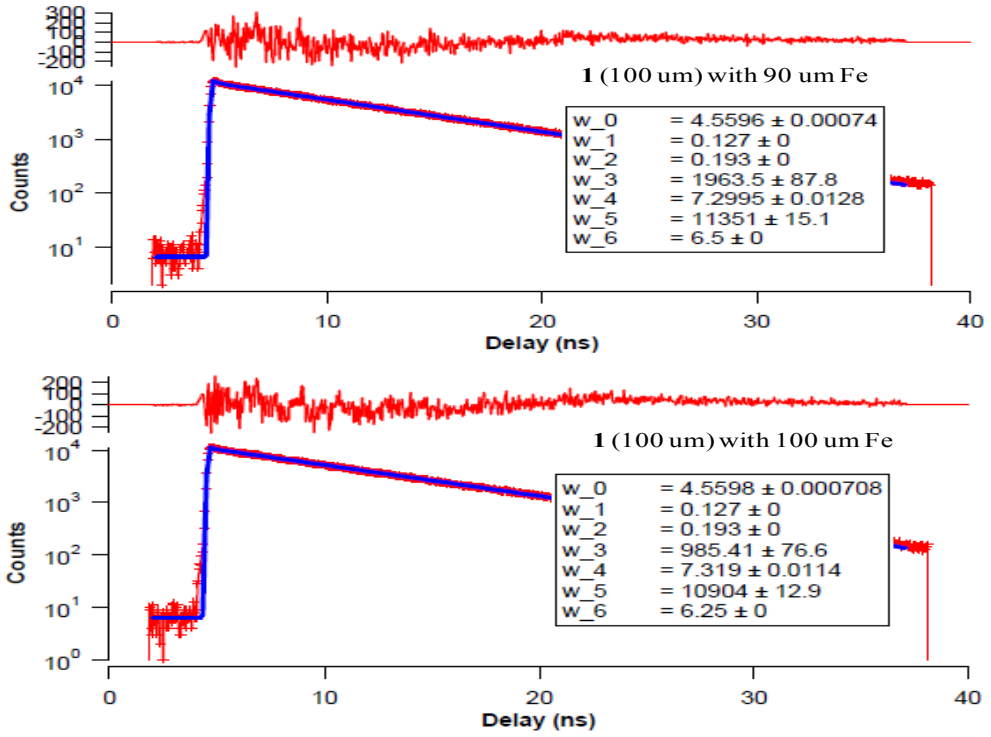

Fig. S11. Nono-second fluorescence decay profile of **1** (100 μM) with 0-100 μM of Fe^{3+} ions (top to bottom)

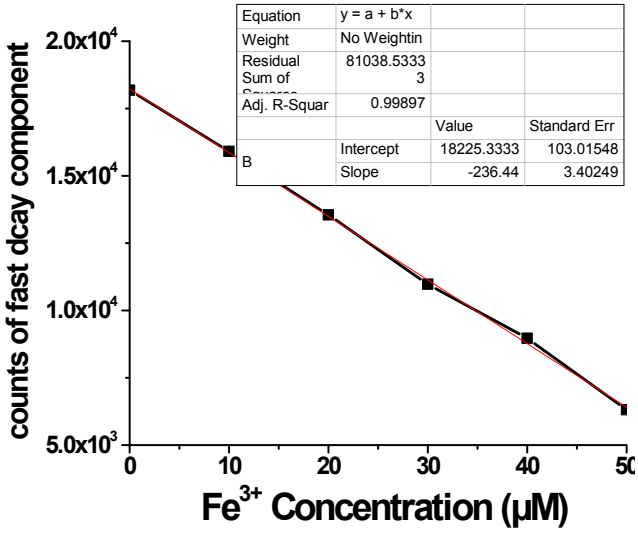

Fig. S12. Linear response curves using the amplitude of fast decay component of **1** to calculate detection limit depending on the Fe^{3+} concentration.

Detection limit = K (SD)/S
Where K = 2 or 3 (we take 3 in this case); SD is the standard deviation of the blank solution; S is the slope of the calibration curve.
The standard deviation of blank in the case of fluorescence lifetime decay experiments is 49.75.

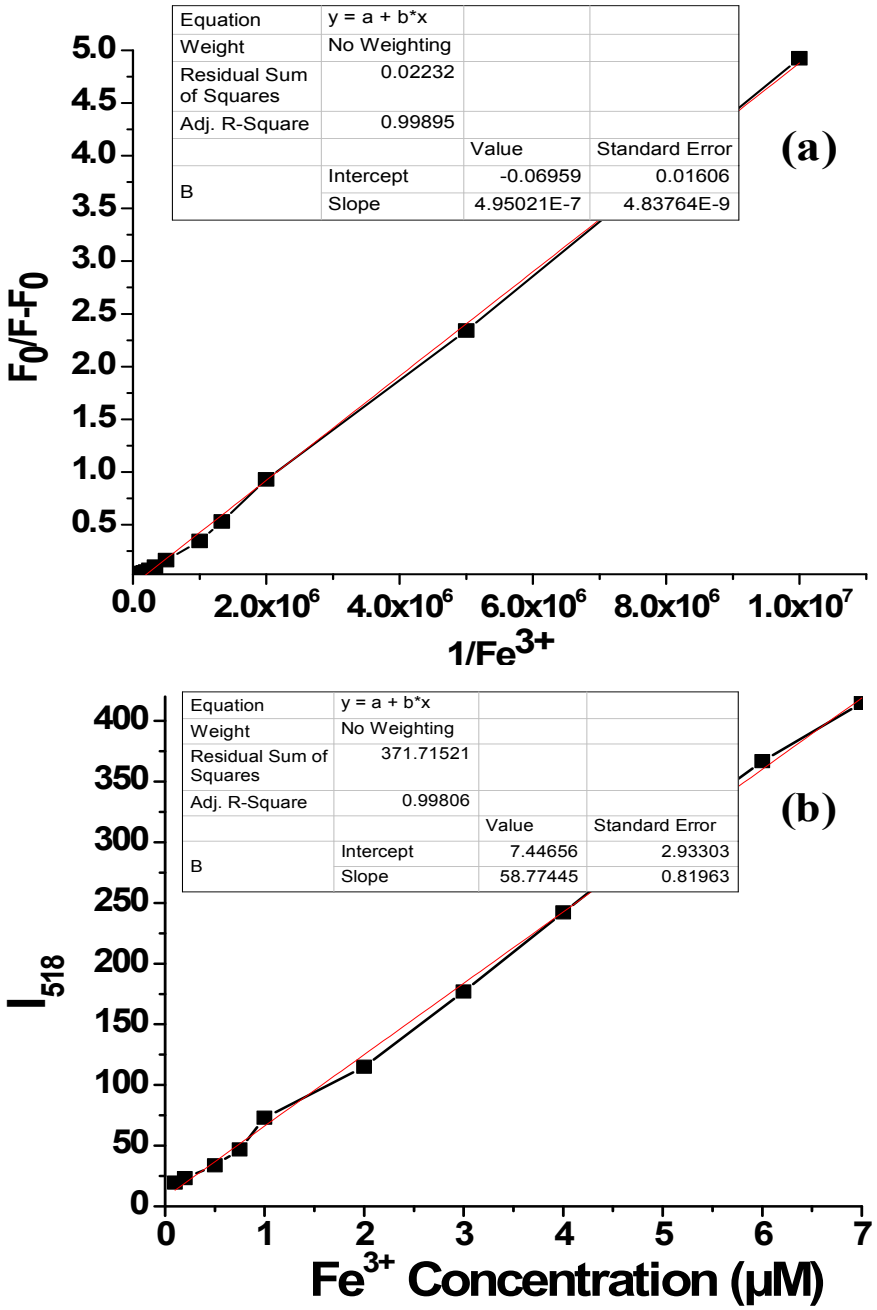

Fig. S13. Benesi–Hildebrand plot for determination of binding constant (**a**) and linear response curves of **1** at 518 nm to calculate detection limit (**b**) depending on the Fe^{3+} concentration.

Binding constant = Intercept/Slope
Detection limit = K (SD)/S
Where K = 2 or 3 (we take 3 in this case); SD is the standard deviation of the blank solution; S is the slope of the calibration curve.
The standard deviation of blank in the case of fluorescence experiments is 0.0602.

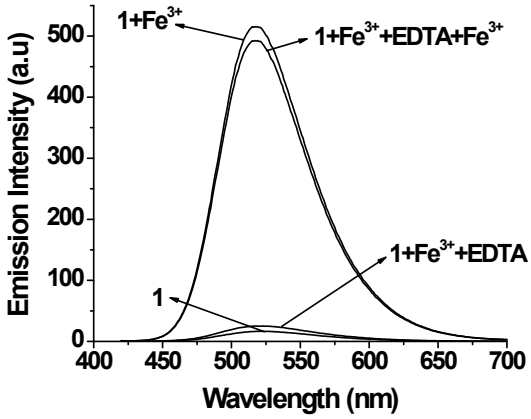

Fig. S14. EDTA experiments to confirm the reversibility of **1**-Fe^{3+} complex

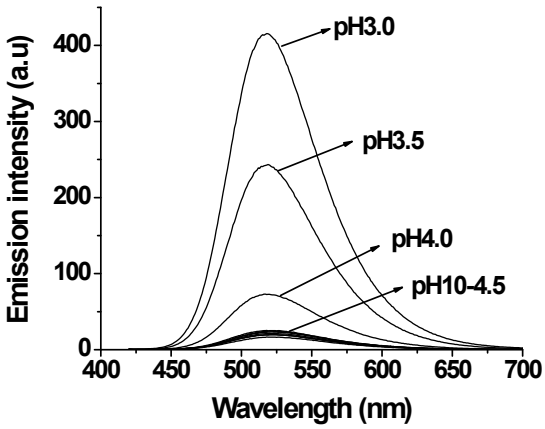

Fig. S15. pH dependant variation in emission intensity of **1** (10 μM) at 518 nm.

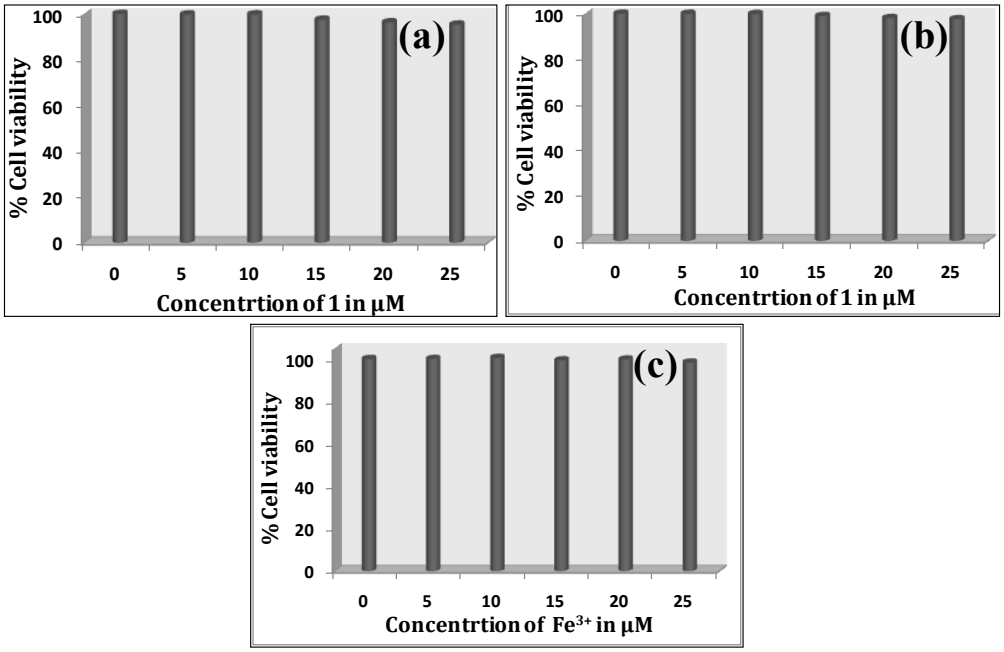

Fig. S16. The cell viability percentage of NIH 3T3 (**a**) and W138 (**b**) cells after treatment with different concentrations of sensor **1** and cell viability percentage of W138 cells after treatment with different concentrations of Fe^{3+} ions (**c**).

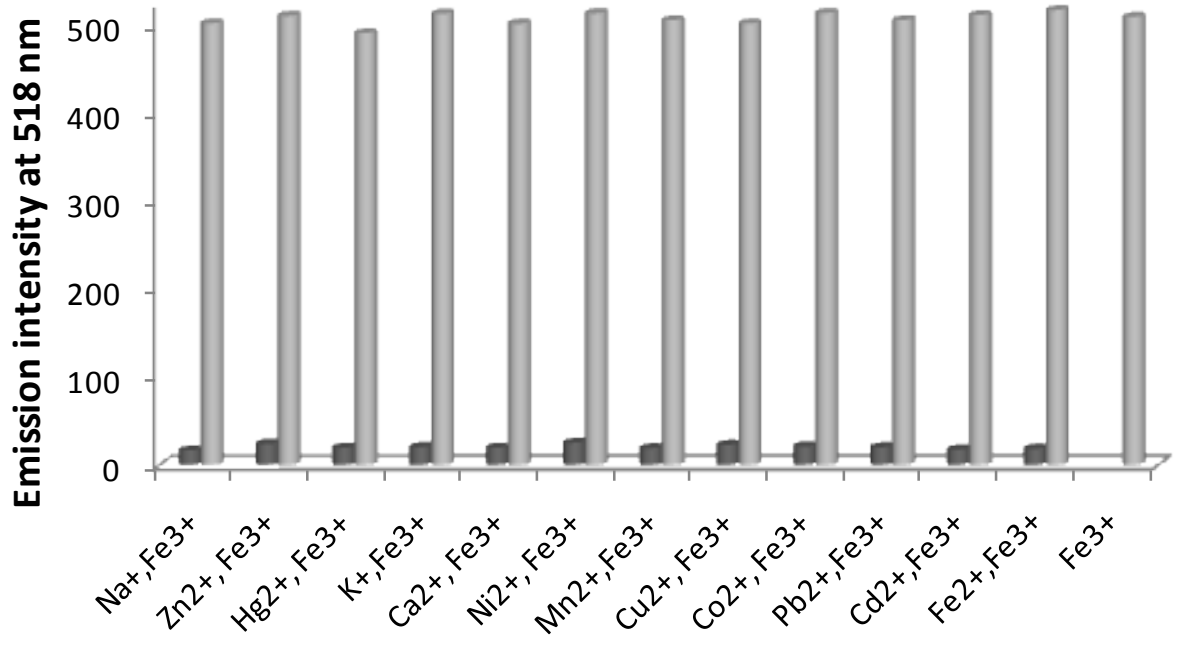

Fig. S17. Metal-ion selectivity of **1** in 1:1 v/v 0.01M Tris HCl-CH_3CN, pH 7.4. The dark bars represent the fluorescence emission at ~518 nm of a solution of **1** (10 μM) and 2 equiv of other metal ions. The light bars show the fluorescence emission at ~518 nm after the addition of Fe^{3+} (10 μM).

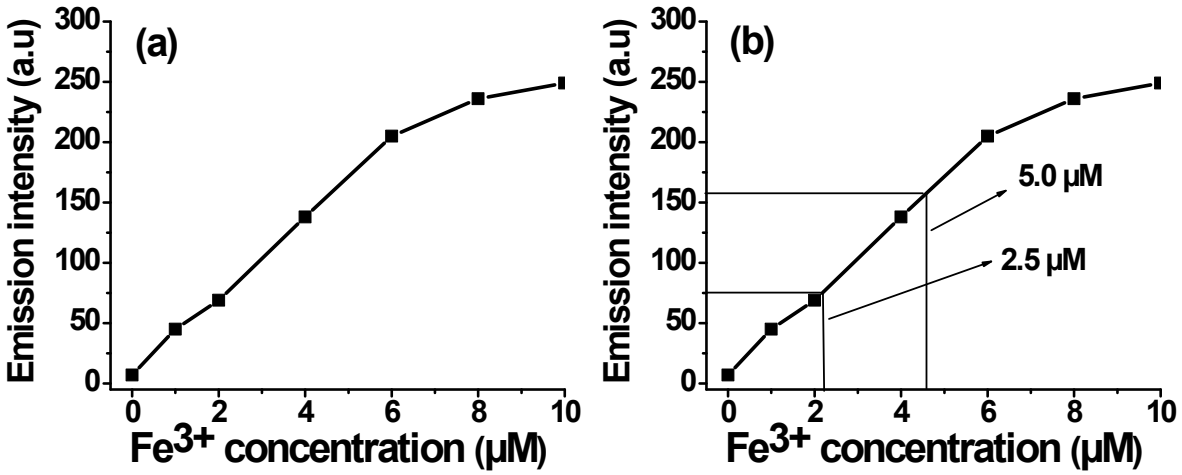

Fig. S18. Plot of the fluorescence emission intensity at 515 nm observed from the W138 cells loaded with **1** (10 μM) upon addition of serial concentration of Fe^{3+} ions measured using well plate reader Vs concentration of Fe^{3+} ions added (**a**) and determination of the amount of Fe^{3+} ions added using calibration curve (**b**).

Table 2: Concentration of Fe^{3+} added to W138 cells measured using fluorescence and ICP-OES methods

Added Fe^{3+} concentration µM (ppm)	**Fe^{3+} concentration measured using**	
	Fluorescence method µM (ppm)	**ICP-OES method µM (ppm)**
2.5 (0.14)	2.2 (0.12)	3.2 (0.18)
5.0 (0.28)	4.6 (0.26)	5.7 (0.32)

References:

1. Gaussian 03, Revision D.01, M. J. Frisch, G. W. Trucks, H. B. Schlegel, G. E. Scuseria, M. A. Robb, J. R. Cheeseman, J. A. Montgomery, Jr., T. Vreven, K. N. Kudin, J. C. Burant, J. M. Millam, S. S. Iyengar, J. Tomasi, V. Barone, B. Mennucci, M. Cossi, G. Scalmani, N. Rega, G. A. Petersson, H. Nakatsuji, M. Hada, M. Ehara, K. Toyota, R. Fukuda, J. Hasegawa, M. Ishida, T. Nakajima, Y. Honda, O. Kitao, H. Nakai, M. Klene, X. Li, J. E. Knox, H. P. Hratchian, J. B. Cross, V. Bakken, C. Adamo, J. Jaramillo, R. Gomperts, R. E. Stratmann, O. Yazyev, A. J. Austin, R. Cammi, C. Pomelli, J. W. Ochterski, P. Y. Ayala, K. Morokuma, G. A. Voth, P. Salvador, J. J. Dannenberg, V. G. Zakrzewski, S. Dapprich, A. D. Daniels, M. C. Strain, O. Farkas, D. K. Malick, A. D. Rabuck, K. Raghavachari, J. B. Foresman, J. V. Ortiz, Q. Cui, A. G. Baboul, S. Clifford, J. Cioslowski, B. B. Stefanov, G. Liu, A. Liashenko, P. Piskorz, I. Komaromi, R. L. Martin, D. J. Fox, T. Keith, M. A. Al-Laham, C. Y. Peng, A. Nanayakkara, M. Challacombe, P. M. W. Gill, B. Johnson, W. Chen, M. W. Wong, C. Gonzalez, and J. A. Pople, Gaussian, Inc., Wallingford CT, 2004.
2. A. D. Becke, *J. Chem. Phys.*, 1993, **98**, 5648.
3. X. Wang, X. Ma, Z. Yang, Z. Zhang, J. Wen, Z. Geng and Z. Wang, *Chem. Commun.*, 2013, **49**, 11263.